



microRNA expression patterns in tumor infiltrating lymphocytes are strongly associated with response to adoptive cell transfer therapy

Gilli Galore-Haskel¹ · Eyal Greenberg¹ · Inbal Yahav² · Etti Markovits^{1,3} · Rona Ortenberg¹ · Ronnie Shapira-Fromer¹ · Orit Itzhaki¹ · Jacob Schachter^{1,4} · Michal J. Besser^{1,3} · Gal Markel^{1,3}

Received: 25 April 2020 / Accepted: 24 October 2020
© Springer-Verlag GmbH Germany, part of Springer Nature 2020

Abstract

Adoptive cell transfer (ACT) using autologous tumor infiltrating lymphocytes (TILs) was previously shown to yield clinical response in metastatic melanoma patients as an advanced line. Unfortunately, there is no reliable marker for predicting who will benefit from the treatment. We analyzed TIL samples from the infusion bags used for treatment of 57 metastatic melanoma patients and compared their microRNA profiles. The discovery cohort included six responding patients and seven patients with progressive disease, as defined by RECIST1.1. High throughput analysis with NanoString nCounter demonstrated significantly higher levels of miR-34a-5p and miR-22-3p among TIL from non-responders. These results were validated in TIL infusion bag samples from an independent cohort of 44 patients, using qRT-PCR of the individual microRNAs. Using classification trees, a data-driven predictive model for response was built, based on the level of expression of these microRNAs. Patients that achieved stable disease were classified with responders, setting apart the patients with progressive disease. Moreover, the expression levels of miR-34a-5p in the infused TIL created distinct survival groups, which strongly supports its role as a potential biomarker for TIL-ACT therapy. Indeed, when tested against autologous melanoma cells, miR^{Low} TIL cultures exhibited significantly higher cytotoxic activity than miR^{High} TIL cultures, and expressed features of terminally exhausted effectors. Finally, overexpression of miR-34a-5p or miR-22-3p in TIL inhibited their cytotoxic ability in vitro. Overall, we show that a two-microRNA signature correlates with failure of TIL-ACT therapy and survival in melanoma patients.

Keywords ACT · microRNA · TIL · Melanoma · Biomarker

Michal J. Besser and Gal Markel have contributed equally to this work.

Electronic supplementary material The online version of this article (<https://doi.org/10.1007/s00262-020-02782-7>) contains supplementary material, which is available to authorized users.

✉ Gal Markel
gal.markel@sheba.health.gov.il

- ¹ Ella Lemelbaum Institute of Immuno-Oncology, Sheba Medical Center, Ramat Gan 526260, Israel
- ² Graduate School of Business Administration, Tel Aviv University, Tel Aviv, Israel
- ³ Department of Clinical Microbiology and Immunology, Sackler Faculty of Medicine, Tel Aviv University, Tel Aviv, Israel
- ⁴ Sackler School of Medicine and Tel Aviv University, Tel Aviv, Israel

Introduction

Melanoma is considered as an immunogenic tumor, expressing a variety of tumor associated antigens [1] and highest mutational burden [2]. Indeed, this field was the first to enjoy the wave of new immunotherapeutic strategies [3, 4]. In 2011, ipilimumab, and antibody blocking cytotoxic T lymphocyte-associated protein 4 (CTLA-4) was approved for the treatment of metastatic melanoma based on survival benefit in randomized Phase III clinical trials [5, 6]. Antibodies that target Program cell Death 1 (PD-1) [7, 8] showed impressive clinical effects, leading to regulatory approvals of pembrolizumab and nivolumab for the treatment of metastatic melanoma and recently in the adjuvant setting. Combination of ipilimumab and PD-1 blockade yields more than 50% response, but with very high toxicity [9]. Inhibitors for additional immune checkpoints are under development, such as: T-cell membrane protein 3 (TIM3), Lymphocyte-activation

gene 3 (LAG3) [10] and Carcinoembryonic antigen-related cell adhesion molecule 1 (CEACAM1) [11, 12].

Adoptive cell therapy (ACT) involves the isolation and *ex vivo* expansion of autologous tumor infiltrating lymphocytes (TILs) that are then infused in combination with IL-2 into the cancer patient, who has undergone non-myeloablative lymphodepleting chemotherapy [13]. Several protocols for ACT in melanoma have been developed along the years, including the use of “selected” TILs, based on their IFN γ release or “Young”-unselected TILs [14–16]. Multiple independent TIL trials in metastatic melanoma patients have consistently yielded objective response rates of around 40%, with many of these responses being durable [17–19]. Although this raises great hope, many patients still do not gain any benefit, stressing the need for predictive biomarkers.

MicroRNAs (miRNAs) are short non-coding RNA molecules that post-transcriptionally regulate gene expression by promoting translational repression or transcript degradation [20, 21]. Thousands of mature human miRNAs are annotated and described in miRbase database [22]. As an individual miRNA can simultaneously modulate the expression of even hundreds of different mRNA targets, it is estimated that more than a half of the total human mRNA species are likely to be subjected to miRNA-mediated control [23]. miRNAs are expressed in a tissue-specific manner and play important roles in cell proliferation, apoptosis, differentiation and metabolism [20]. Considering the prevalence of miRNA-mediated gene regulation, alterations in miRNAs expression can significantly contribute to changes in important cellular pathways and thus underlie diseases. Indeed, numerous studies confirm the involvement of miRNAs in autoimmune diseases [24], neurodegenerative diseases [25] and cancer [26–29]. The majority of current studies are focused on miRNA signatures as biomarkers for diagnosis, prognosis or therapeutic response [29, 30].

Here we describe a 2-miRNA signature in the infused TIL, which correlates with response and survival in 57 metastatic melanoma patients treated with TIL-ACT. A proof-of-principle evidence for the effect of these miRNAs on TILs cytotoxic capacity implies on a mechanistic basis.

Materials and methods

Melanoma patients and infusion TIL samples

57 metastatic melanoma patients treated with TIL-ACT immunotherapy at the Ella Lemelbaum Institute of Melanoma at Sheba Medical Center, between years 2008 and 2013 [14, 17] were included in the study. All TIL treatments were based on the “Young” TIL protocol, except for four patients who were treated with the “Selected” protocol [14,

17, 31, 32]. Patients’ response was determined according to RECIST v1.1 criteria as progressive disease (PD) patients, stable disease (SD), or responders which included partial (PR) or complete response (CR) patients. The clinical characteristics of all patients in the Discovery and Validation cohorts are detailed in Table 1. All patients gave written informed consent prior to their participation in this study. This study was approved by the Israel Ministry of Health (Helsinki approval no. 3518/2004, NCT00287131).

Cells and media

The melanoma and TIL culture were obtained from surgically excised melanoma specimens at our institute. TILs were cultured as previously described [17]. Melanoma cells were maintained in RPMI-1640 medium (Biological Industries) with supplements and 10% FBS (Biological Industries).

RNA isolation

Total RNA was isolated from post-rapid expansion TILs [31] of melanoma patients prior to infusion, using Tri Reagent (Sigma-Aldrich, Rehovot, Israel), according to manufacturer’s instructions. Samples were run on 1% agarose gel electrophoresis to assess integrity and quantification of RNA was measured by NanoDrop 2000 (Thermo Scientific, Waltham, MA). For analysis of miRNA expression following electroporation, RNA was isolated using miRNeasy Micro-Kit (Qiagen, Hilden, Germany), according to manufacturer’s instructions.

NanoString nCounter miRNA assay

NanoString nCounter_Human_miRNA_Assay_v2 was performed according to manufacturer’s instructions (NanoString Technologies Inc, Seattle, WA). Data was normalized to the top 100 most highly expressed miRNAs in each sample. Background detection threshold was determined based on the mean expression values of six negative control probes in each sample. Values exceeding background detection threshold were considered to be indicative of relevant miRNA expression.

Reverse transcription and quantitative real-time PCR (qRT-PCR)

cDNA was generated using Universal cDNA synthesis kit (Exiqon, Vedbaek.

Denmark). miRNAs expression was tested using MicroRNA LNATM PCR primers (Exiqon). The qRT-PCR reactions were run in triplicates on LightCycler480 system (Roche, Basel, Switzerland). miRNAs transcripts were

Table 1 Clinical data of the Discovery and Validation cohorts

#	Sample ID	TIL Protocol	Response	Age	Sex	Stage	Post TIL therapy lines	Comments
Discovery cohort								
1	14	Selected	CR	53	M	M1c	BioChemo	
2	52	Young	PR	45	M	M1b	N/A	Ongoing (11y)
3	54	Young	CR	66	M	M1c	N/A	Ongoing (10y)
4	56	Young	CR	61	M	M1b	N/A	Ongoing (10y)
5	92	Young	CR	45	M	M1b	N/A	Ongoing (8y)
6	93	Young	PD	54	F	M1c	N/A	
7	95	Young	PD	39	M	M1c	Ipi	
8	96	Young	PD	57	F	M1c	N/A	
9	108	Young	PD	63	M	M1c	DTIC + Bev, Carbo + Pacli, Pidi, IL-2 SC	No response to all post TIL lines
10	111	Young	CR	49	F	M1c	N/A	Ongoing (7.5y)
11	113	Young	PD	62	M	M1c	Carbo + Pacli	
12	125	Young	PD	59	F	M1c	Pidi, Ipi	
13	136	Young	PD	66	F	M1c	TMZ	
Validation cohort								
1	9	Selected	SD	55	M	M1c	N/A	
2	23	Selected	SD	34	M	M1c	N/A	
3	33	Selected	SD	50	M	M1c	N/A	
4	34	Young	PD	36	M	M1c	N/A	
5	39	Young	PR	36	M	M1c	Pacli, Ipi, Vem	
6	41	Young	PD	57	M	M1c	Carbo-Pacli	
7	48	Young	SD	22	M	M1b	Pacli, Sor + TMZ	
8	51	Young	SD	41	F	M1a	Ipi, Vem	
9	53	Young	PD	57	M	M1b	N/A	
10	57	Young	PR	71	M	M1c	N/A	
11	60	Young	PD	68	F	M1c	N/A	
12	66	Young	PR	41	M	M1c	Ipi	
13	71	Young	SD	36	F	M1c	N/A	
14	72	Young	SD	49	M	M1c	Caro + Pacli + Bev	
15	76	Young	SD	29	F	M1c	Ipi	
16	79	Young	SD	48	M	M1c	Ipi	
17	80	Young	PD	43	F	M1c	N/A	
18	81	Young	PR	52	M	M1b	Ipi	
19	82	Young	SD	63	M	M1c	Ipi	
20	85	Young	PR	54	F	M1c	Vem	
21	87	Young	PR	33	M	M1c	Carbo + Pacli, Pidi, Ipi	
22	90	Young	PD	45	F	M1c	Ipi	
23	94	Young	PD	27	F	M1c	Ipi	
24	100	Young	PD	51	F	M1c	N/A	
25	101	Young	SD	53	F	M1c	N/A	
26	103	Young	PD	61	M	M1c	N/A	
27	105	Young	PR	34	M	M1c	N/A	
28	110	Young	PR	66	M	M1c	Ipi	
29	114	Young	SD	32	F	M1c	N/A	
30	115	Young	PR	64	M	M1c	Ipi	
31	120	Young	PD	45	M	M1a	N/A	
32	122	Young	PD	55	M	M1c	N/A	
33	123	Young	PR	54	M	M1c	N/A	Ongoing PR

Table 1 (continued)

#	Sample ID	TIL Protocol	Response	Age	Sex	Stage	Post TIL therapy lines	Comments
34	124	Young	CR	42	M	M1c	Pembro	
35	127	Young	SD	71	M	M1c	Ipi	
36	128	Young	PR	46	F	M1c	N/A	
37	129	Young	PR	36	M	M1c	N/A	Ongoing PR
38	130	Young	PD	28	F	M1c	N/A	
39	131	Young	PD	50	M	M1c	Pembro	
40	132	Young	PD	50	M	M1c	Pembro	
41	133	Young	SD	72	M	M1b	N/A	
42	139	Young	PD	60	F	M1c	Ipi	
43	144	Young	CR	42	F	M1c	N/A	Ongoing CR
44	148	Young	PD	71	M	M1c	N/A	

Patients are organized consecutively and categorized according to response groups. CR, PR, SD and PD stand for complete response, partial response, stable disease and progressive disease, respectively. Age and stage indicated in the table were at time of TIL therapy

Vem Vemurafenib, *Ipi* Ipilimumab, *Pembro* Pembrolizumab, *Pidi* Pidilizumab, *Carbo* Carboplatinum, *Pacli* Paclitaxel, *Bev* Bevacizumab, *TMZ* Temozoloide, *DTIC* Dacarbazine, *Sor* Sorafenib, *SC* Subcutaneous, *N/A* Not applicable

detected using SYBR Green master mix (Exiqon), according to manufacturer's instructions. Reactions were normalized to SNORD48 control (ΔCt). Relative expression was calculated compared to responders group using $2^{(-\Delta\Delta Ct)}$ equation, as previously described [33].

Flow cytometry

Expression of cell surface proteins on TIL cultures was determined by flow cytometry. The following antibodies were used for flow cytometry: PE-labeled antihuman CD3 (Cat. no. 555340 BD Bioscience), FITC-labeled antihuman CD4 (Cat. no. 110049, eBioscience), PerCP-labeled antihuman CD8 (Cat. no. 345774, BD Bioscience) or PE-Cy7-labeled antihuman CD8 (Cat. no. 344712, BioLegend), APC-labeled antihuman CD25 (Cat. no. 170259, eBioscience), APC-labeled antihuman CD27 (Cat. no. 170279, eBioscience), PE-labeled antihuman CD62L (Cat. no. 120629, eBioscience), APC-labeled antihuman CXCR3 (Cat. no. FAB160A, R&D), FITC-labeled antihuman CD28 (Cat. no. 110289, eBioscience), APC-labeled antihuman CD69 (Cat. no. 170699, eBioscience), PE-labeled antihuman GITR (Cat. no. FAB689P, R&D) and PE-labeled antihuman OX40 (Cat. no. FAB3388P, R&D). TIL were washed and re-suspended in FACS buffer consisting of 0.5% BSA in PBS. Cells were incubated for 30 min with the antibodies on ice, washed in FACS buffer, and read as the relative log fluorescence of live cells using FACS Calibur flow cytometer (BD Bioscience). Samples were analyzed using FlowJo software (BD Bioscience). Cells were gated on viable lymphocytes, according to FSC and SSC, as well as singlets. The cells

were further gated on CD3 + T cells, and a representative gating strategy figure is shown in Supplementary Fig. 1.

miRNA electroporation

TILs were washed with OPTI-MEM (Thermo Fisher Scientific) and re-suspended in OPTI-MEM at 1×10^6 cells/50 μ l. Cells were electroporated using BTX ECM830 (Harvard Apparatus, Holliston, MA) at 400 V for 1 ms with a total of 4 μ M miScript miRNA Mimics (miR-34a-5p + Negative Control, miR-22-3p + Negative Control, miR-34a-5p + miR-22-3p or Negative Control only (Qiagen)) in a 2-mm cuvette (Harvard Apparatus). Cells and cuvettes were pre-chilled by putting them on ice for 20 min before electroporation. Immediately after electroporation, cells were transferred to fresh pre-warmed complete medium [31] and incubated at 37 °C. After 2 h, cells were washed twice, counted and seeded for cytotoxicity assays.

LDH cytotoxicity and total cell number assays

miRNA electroporated TILs (6×10^4 cells/well) were used as effectors and seeded in 96-well plate and incubated for 72 h. Then, 8×10^3 target cells were added and co-incubated for 18 h. Fresh medium was added to the rest of the wells. Lactate dehydrogenase (LDH) release was measured in the supernatant with CytoTox 96 (Promega, Madison, WI) according to manufacturer's instructions using a microplate reader (GloMax, Promega, Madison, WI) at 490 nm. Experiments were performed in quadruplicate wells. Percent of specific lysis of target cells was calculated using the equation: $(\text{Experimental} - \text{Effector}_{\text{Spontaneous}} - \text{Target}_{\text{Spontaneous}}) /$

$(\text{Target}_{\text{Maximum}} - \text{Target}_{\text{Spontaneous}}) \times 100$. Maximum LDH release of effector cells was used to normalize for differences in total cell numbers counts between electroporated TILs. To ensure linearity of the LDH cytotoxicity assay, a standard curve consisting of different Effector:Target (E:T) ratios was generated by co-incubating different amounts of melanoma from patient #14 (mel14) with fixed amounts of corresponding TIL (TIL14). The assay was performed as described above.

RNA sequencing

RNA from TIL products of advanced melanoma patients was extracted with Tri Reagent (Sigma-Aldrich, Cat#T9424) according to manufacturer protocol. RNA-seq libraries were prepared with Illumina's Ribo Zero Gold and TruSeq stranded library prep kits and sequenced on the Illumina HiSeq 2500 platform using paired-end sequencing with read length of 2×125 –150 bps. Reads were aligned to the human genome reference build hg38 using STAR aligner [34] and were quantified with FeatureCounts [35]. After filtration of lowly expressed genes (counts below 10 in more than 90% of samples), raw counts were normalized and analyzed in the R environment according to the LIMMA pipeline [36, 37]. Transcriptomes of miR-high and low TIL products were compared using the R package LIMMA pipeline. The cytolytic score was calculated by the geometric mean of GMZA and PRF1 [38]. Normalized gene expression of immune checkpoints and T-cell state markers was visualized using the R package pheatmap.

Statistical analysis

NanoString data analysis was performed by calculating the fold change between the mean expression of responding patients and the mean expression of PD patients, for each miRNA. *P* value was calculated using the unpaired two-tailed Student's *t* test. Differentially expressed miRNAs were selected based on the following criteria: $p \leq 0.05$ and fold change ≤ 0.66 or ≥ 1.5 .

Significance of variation between groups was evaluated using the unpaired two-tailed Student's *t* test, Mann–Whitney test, ANOVA or proportion test.

A classification tree with *k*-fold validation method was carried to distinguish responders from non-responders based on patients' miRNA expression levels. Three approaches were examined: (1) differentiation of responders (CR + PR) from non-responders (SD + PD). This approach treats SD patients as non-responders, since these patients do not exhibit any objective response; (2) exclusion of SD patients from the classification analysis and re-add them in the prediction stage; (3) regarding SD as Clinical Benefit together with the CR + PR. It should be emphasized that the splits in

the classification trees are data driven, similar to coefficients of regression model, and are not arbitrary user-determined “cut-offs”. Splits were determined by conditional inference using a Chi squared test [39]. Thus, splits are pre-ROC curves, and leaves in the tree are used to determine the probability (= proportion in the leaves) of an observation to be classified as a responder or non-responder. Kaplan–Meier analysis for survival was performed on the terminal nodes of the best classification tree models. All *p* values were two-sided and statistical significance was set at $p \leq 0.05$.

microRNA bioinformatics

We utilized TargetScan (<http://www.targetscan.org/>) to identify predicted targets of miRNAs and Toppgene (<https://toppgene.cchmc.org/enrichment.jsp>) algorithm for pathway analysis.

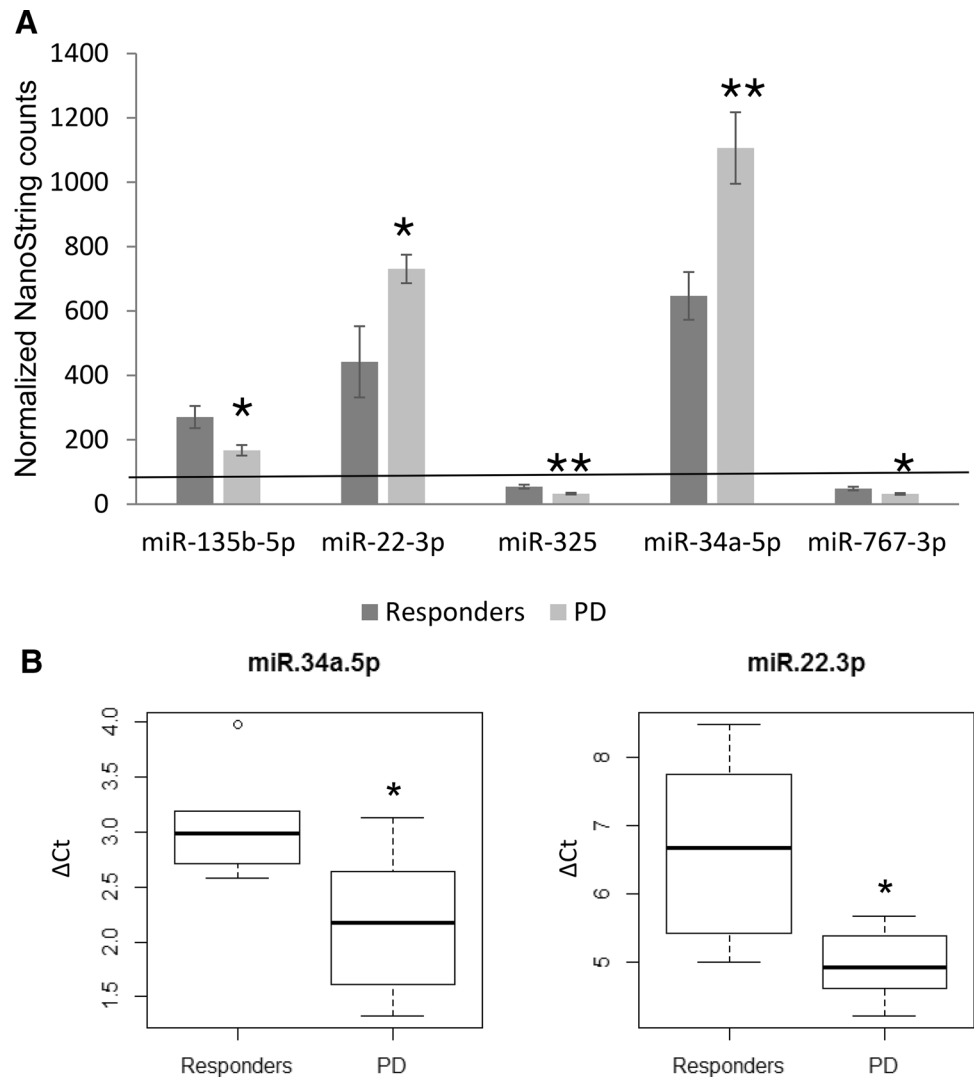
Results

miRNA expression in TIL-ACT treated patients

The discovery cohort, comprised of 7 PD patients (3 males; mean age 57.2) and 6 responders (5 CR patients and 1 PR patient with over 5 years of progression free survival; 5 males; mean age 53.2) was screened for 800 miRNAs using NanoString nCounter Human miRNA assay. The cohort compares extreme clinical outcomes, and we hypothesized it will highlight major potential differences. This screen yielded 5 differentially expressed miRNAs, with only 3 of them—miR-34a-5p, miR-22-3p and miR-135b-5p showing values exceeding background detection threshold, as shown in Fig. 1a. Since overall expression levels of miR-135b-5p were relatively low, we decided to concentrate on miR-34a-5p and miR-22-3p. The results of these two miRNAs were validated technically using qRT-PCR as another method (Fig. 1b, detailed depiction of miR-34a-5p and miR-22-3p values appears in Supplementary Table 1).

miR-34a-5p and miR-22-3p expression was further validated by qRT-PCR in a validation cohort of 44 patients comprised of 16 PD, 14 SD, 12 PR and 2 CR patients. Clinical data of all patients, including the discovery cohort, is detailed in Table 1. Within the discovery cohort, there was no significant difference between responders group (CR + PR) and PD patients regarding age, number of IL-2 doses administered during TIL treatment and LDH values, and a significant difference in BRAF mutation status (Fig. 2a, detailed in Supplementary Table 1). Response was associated in a statistically significant manner with high CD27 and low CD25 frequencies, and a similar trend was also observed for high CD8 frequency as measured with flow cytometry (Fig. 2b, detailed depiction of tested markers

Fig. 1 Differentially expressed miRNAs in the discovery cohort. **a** NanoString nCounter Human miRNA Assay was performed to profile microRNAs expression in TIL-ACT treated patients—6 responders (5 CR and 1 PR patients) and 7 PD patients. Differentially expressed miRNAs (out of 800 miRNAs analyzed) were selected based on the criteria of $p \leq 0.05$ and fold change ≤ 0.66 or ≥ 1.5 . Normalized Nanostring counts are shown for each group. Black horizontal line indicates background detection threshold; **b** miR34a-5p and miR-22-3p expression levels were assessed by qRT-PCR and normalized to SNORD48 expression in responders and PD patients. Box plots of ΔCt values are shown for each miRNA. As such, lower values indicate higher expression



appears in Supplementary Table 1). In the validation cohort, Responders, Stable Disease and Progressive Disease groups were compared. None of the clinical parameters or the T cell markers were associated with response (Fig. 2c, d). In line with the results of the discovery cohort, a trend for association with response was observed for high frequency of CD8, and a trend for association with progressive disease was observed for high CD25 frequency (Fig. 2d). In addition, a trend for association of high frequency of CD4 with progressive disease was observed (Fig. 2d). Finally, there were no significant differences in any of these parameters between the discovery and validation cohorts. No correlation was observed between the percentage of CD8+ T cells in the infusion bag and the expression level of miR-34a-5p ($r=0.12$) or miR-22-3p ($r=0.32$) (Supplementary Fig. 2). The progression free survival (PFS) and overall survival (OS) of all 57 patients grouped according to their response to therapy (Fig. 2e, f), and concur with previously published data [17–19]. Noteworthy, PFS of SD patients was similar to

PD patients, but their OS was significantly better (Fig. 2e, f). This difference could not be explained by subsequent post TIL therapy, as both groups received similar treatments: 7 of the 14 SD patients received post TIL therapy (5 of them received Ipilimumab), and 11 of the 23 PD patients received post TIL therapy (8 of them received Immune checkpoint inhibitors such as ipilimumab, pembrolizumab, or pidilizumab) (Table 1).

Multivariate analysis on this limited dataset carries a risk of overfitting. No stable model that can be generalized out-of-sample was available to predict responders. When SD are excluded, miR-34a is the top predictor. The next important predictors are miR-22, CD4 and CD8. The order between them changes across training samples. The best predictors of clinical benefit were miR-34a and miR-22, followed by CD4. We, therefore, used conditional inference trees on the entire set of variables. When predicting clinical benefit, we receive a 2-level tree, split on miR-34a. Other outcomes resulted in a singleton tree (no splits). Notably, trees are

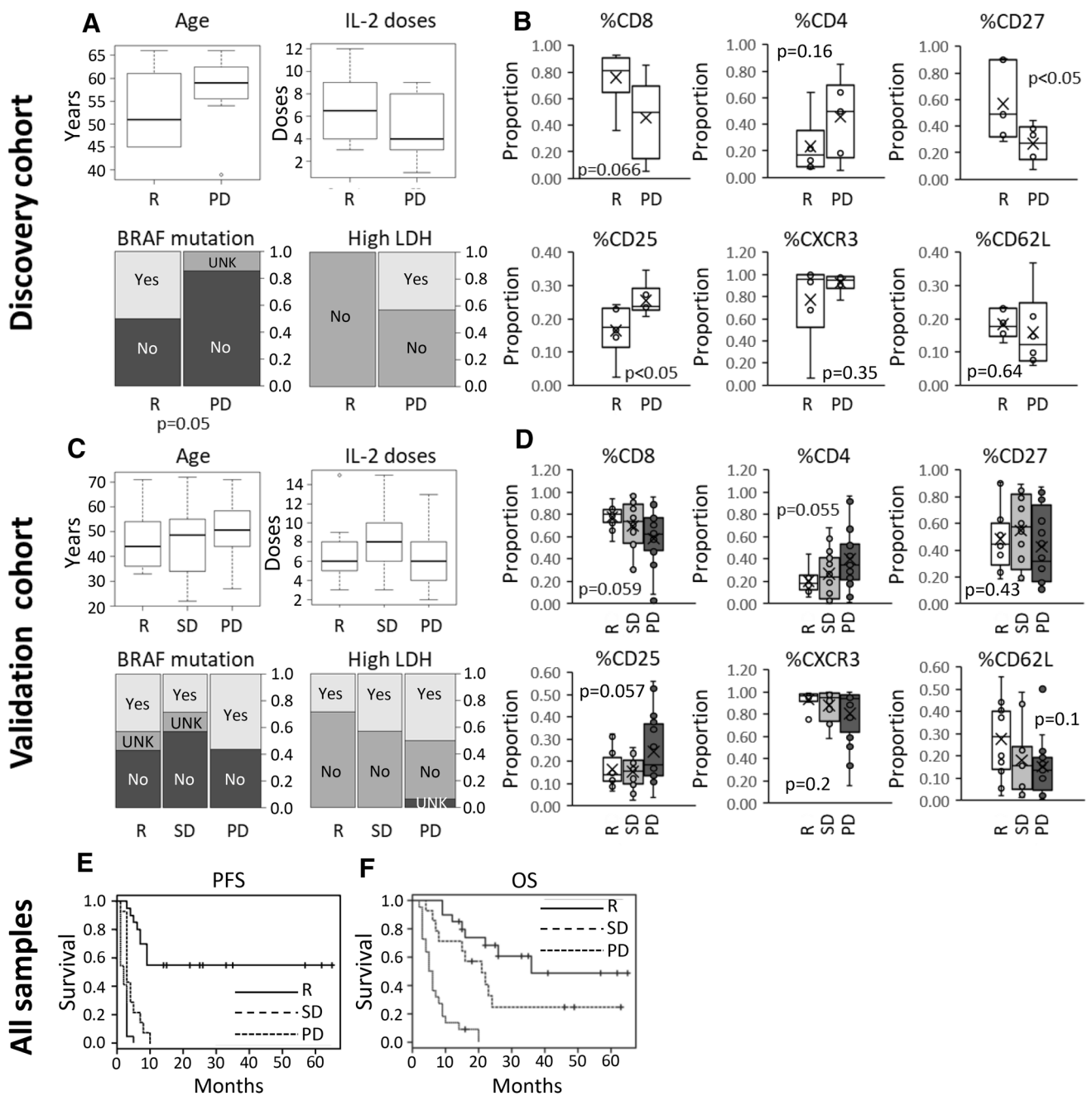


Fig. 2 Clinical data of the discovery and validation cohorts. Data was categorized by Discovery and Validation cohorts, as indicated in the figure. **a** and **c** depict clinical characteristics including age, number of IL-2 doses administered during TIL treatment, BRAF mutation and whether high LDH levels; **b** and **d** depict the percentage of different T-cell markers in the T-cell product from the infusion bags; **e**

describes the progression free survival and **f** overall survival of the combined cohorts, according to clinical response to TIL. Statistical tests used were Chi square for categorical variables, *t* test and ANOVA for quantitative variables. The *p* values are indicated in the figure. R—Responders, PD—Progressive Disease, SD—Stable Disease, PFS—Progression-Free Survival, OS—Overall Survival

corrected to multiple tests, thus the threshold for significance is negatively correlated with the number of variables. With small data, this limitation is likely to result in singleton trees. Therefore, we further ran a conditional inference tree on the top variables extracted from the random forest model: miR-34a, miR-22, CD4, CD8. While the resulted trees vary across

samples, miR-34a consistently split the trees fit for response excluding SD, and for clinical benefit, which includes SD.

Analysis of the integrated cohorts (total 57 patients) showed that miR-34a-5p and miR-22-3p were both up-regulated in the PD patients compared to the responders group and displayed a very high correlation ($\rho = 0.728$;

$p = 1.38 \times 10^{-10}$): 1.46-fold change for miR-34a-5p ($p=0.004$) and 1.87-fold change for miR-22-3p ($p=0.003$), while no difference was observed between SD patients and the responders group (0.94-fold change, $p=0.6$ and 0.95-fold change, $p=0.8$ for miR-34a-5p and miR-22-3p, respectively). Statistically significant differences in ΔCt values of miR-34a-5p ($p=0.04$) and miR-22-3p ($p=0.05$) were observed between the responders group and PD patients (Fig. 3a). When SD patients were grouped together with PD patients (i.e., non-responders), no statistically significant difference was observed in ΔCt values of the miRNAs compared to responders (Fig. 3b; miR-34-5p $p=0.58$ and miR-22-3p $p=0.71$). However, when SD patients were grouped together with the responders group (i.e., clinical benefit), statistically significant difference was observed (Fig. 3c; miR-34-5p $p=4 \times 10^{-3}$ and miR-22-3p $p=8 \times 10^{-3}$). These results suggest that miR-34a-5p and miR-22-3p expression in TILs can differentiate between patients with and without clinical benefit from TIL-ACT treatment. This concurs with the different overall survival of SD patients from PD patients (Fig. 2f).

miR-34a-5p and miR-22-3p expression correspond with response and survival

Random Forest analysis of 500 trees fit to different samples of the data were generated, and the importance of each predictor to the model accuracy was aggregated over the trees. In the first approach (responders = (CR + PR); non-responders = (SD + PD)), the classification tree yields an empty decision model, implying that there are no statistical differences between the responders and non-responders groups in terms of miR-34a-5p and miR-22-3p expression level. In the second (responders = (CR + PR); non-responders = (PD); SD excluded, therefore, $n=43$) and third approaches (clinical benefit = (SD + CR + PR); non-clinical benefit = (PD), therefore, $n=57$), the classification trees distinguishes responders/clinical benefit from non-responders/non-clinical benefit based on their miR-34a-5p (Fig. 4a) and miR-22-3p (Fig. 4b) expression levels.

We next ran conditional inference trees on the entire set of variables. When predicting clinical benefit, we receive a 2-level tree, split on miR-34a. Other outcomes result in a singleton tree (no splits). However, as trees are corrected to multiple tests, the threshold for significance is negatively correlated with the number of variables. With small data, this limitation is likely to result in singleton trees. To overcome this limitation, we further ran a Conditional Inference tree on the top variables extracted from the random forest model: miR-34a, miR-22, CD4 and CD8. While the resulted trees vary across samples, miR-34a consistently splits the trees fit for response excludes SD and for clinical benefit.

Due to the high correlation between the miRNAs (0.728, $p < 0.00001$, Fig. 4c), these decision trees are interchangeable, meaning that either miRNA can be potentially used for classification, and the marginal contribution of one miRNA over the other is negligible.

The prediction accuracies of the trees 1 and 2 are given by the confusion matrices in Fig. 4a, b, respectively. The matrices show the model classification compared to the actual patients groups (CR, PR, SD, PD). The first tree, split by miR-34a-5p, is shown to better distinguish PD patients from the other three groups (CR, PR, SD). The classification corresponds to cutoff value of 0.5. It should be noted that to determine a cutoff value, the data must be split into 3 sets: training (for model fitting), validation (for cutoff tuning), and test (for evaluation) [40], which is not feasible with the number of samples available ($n=57$). Both trees were found to have only a single split (left or right leaf), and in all cases the proportions are close to either 0 or 1 (Fig. 4a, b). This concludes into a 2-piece linear ROC curve (Fig. 4d), implying that any cutoff in the mid-range would result in the same classification, and that the cutoff value of 0.5 is optimal for the data, as the only other alternative is to classify all observations as either responders or non-responders.

Interestingly, under both models, SD patients are classified as responders. This observation validates the approach to exclude SD patients from the analysis (or else, consider them together with responders). Under this approach, the most accurate model is given by the first tree. Whereas the type I error rate for this model is fairly high (0.52), the type II error rate is extremely low (0.05) with a strong Negative Predictive Value of 91.7%. That is, the model accurately predicts non-responders.

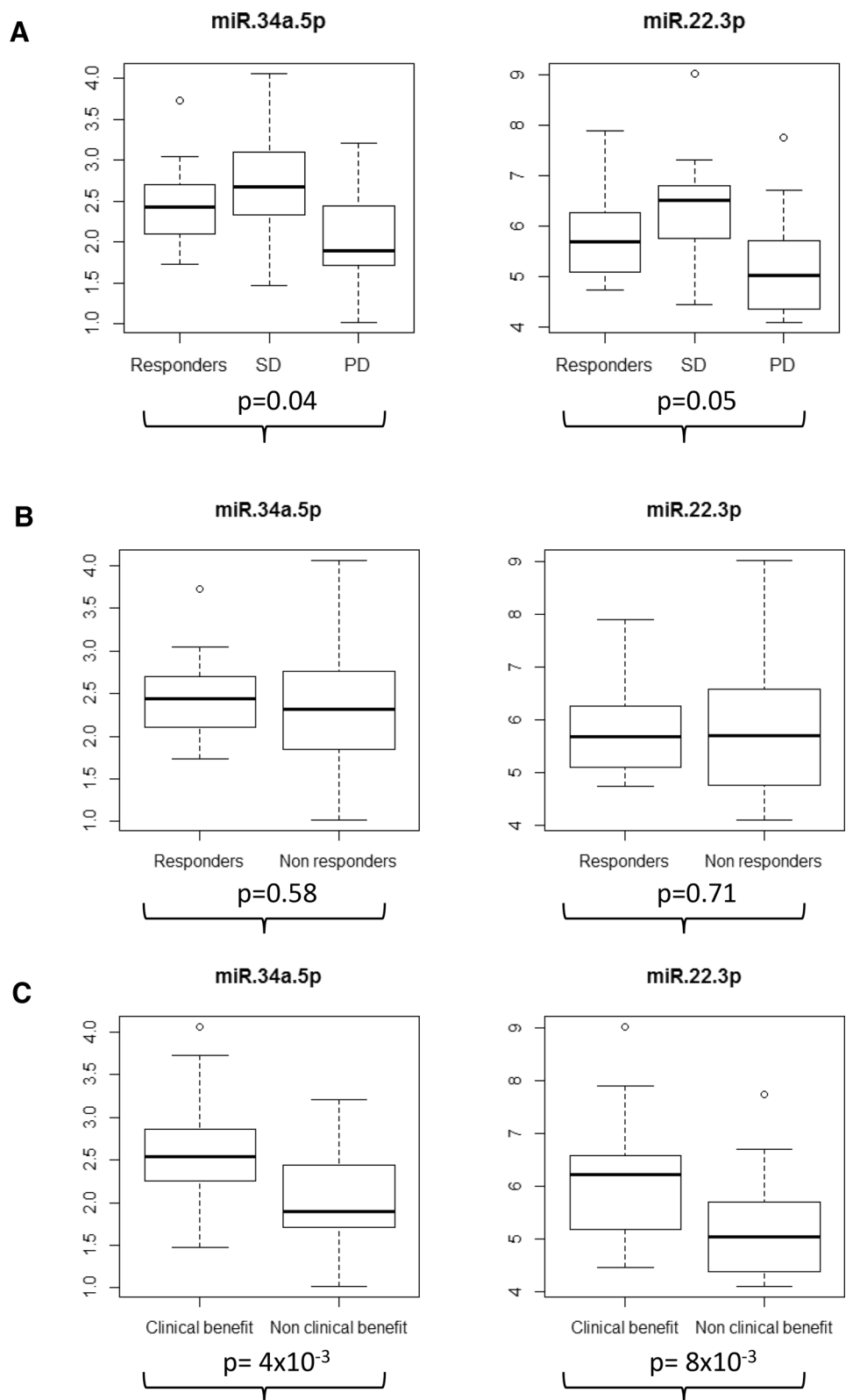
OS was measured from TIL infusion to death and PFS was measured from TIL infusion to documented disease progression or death. Kaplan–Meier OS and PFS analysis on the terminal nodes of trees 4A and 4B are given in Fig. 4e, f. Patients with low expression of miR-34a-5p ($\Delta\text{Ct} > 1.85$) showed significantly increased OS ($p=0.003$) and PFS ($p=0.001$) than patients with high expression ($\Delta\text{Ct} < 1.85$) of the miRNA. No difference was observed in OS ($p=0.17$) and PFS ($p=0.19$) between patients with low expression ($\Delta\text{Ct} > 5.67$) or high expression ($\Delta\text{Ct} < 5.67$) of the miR-22-3p.

These results suggest that miR-34a-5p may serve as markers for predicting response and prognosis to TIL-ACT and that SD patients are considered as clinical benefit based on their miR-34a-5p expression levels.

miR-34a-5p and miR-22-3p regulate T cells cytotoxicity

We analyzed the phenotype and function of four TIL cultures with high expression of miR-22-3p and miR-34a-5p

Fig. 3 miR-34a-5p and miR-22-3p expression differentiates between patients with and without clinical benefit from TIL-ACT. miR34a-5p and miR-22-3p expression levels were assessed by qRT-PCR and normalized to SNORD48 expression. Box plots of ΔC_t values are shown for each miR in **a** responders (CR+PR), SD and PD patients; **b** responders (PR+CR) vs. non responders (SD+PD) patients; **c** clinical benefit (PR+CR+SD) vs. non-clinical benefit (PD) patients



(miR-High), and four with low expression of these microRNAs (miR-Low). The miR-High group expressed 5.1-fold and 2.5-fold of miR-22-3p and miR-34a-5p, respectively,

than the miR-Low group (Supplementary Table 2). The miR-High group had a statistically significant higher proportion of CD27 and a trend for higher CD8, as measured

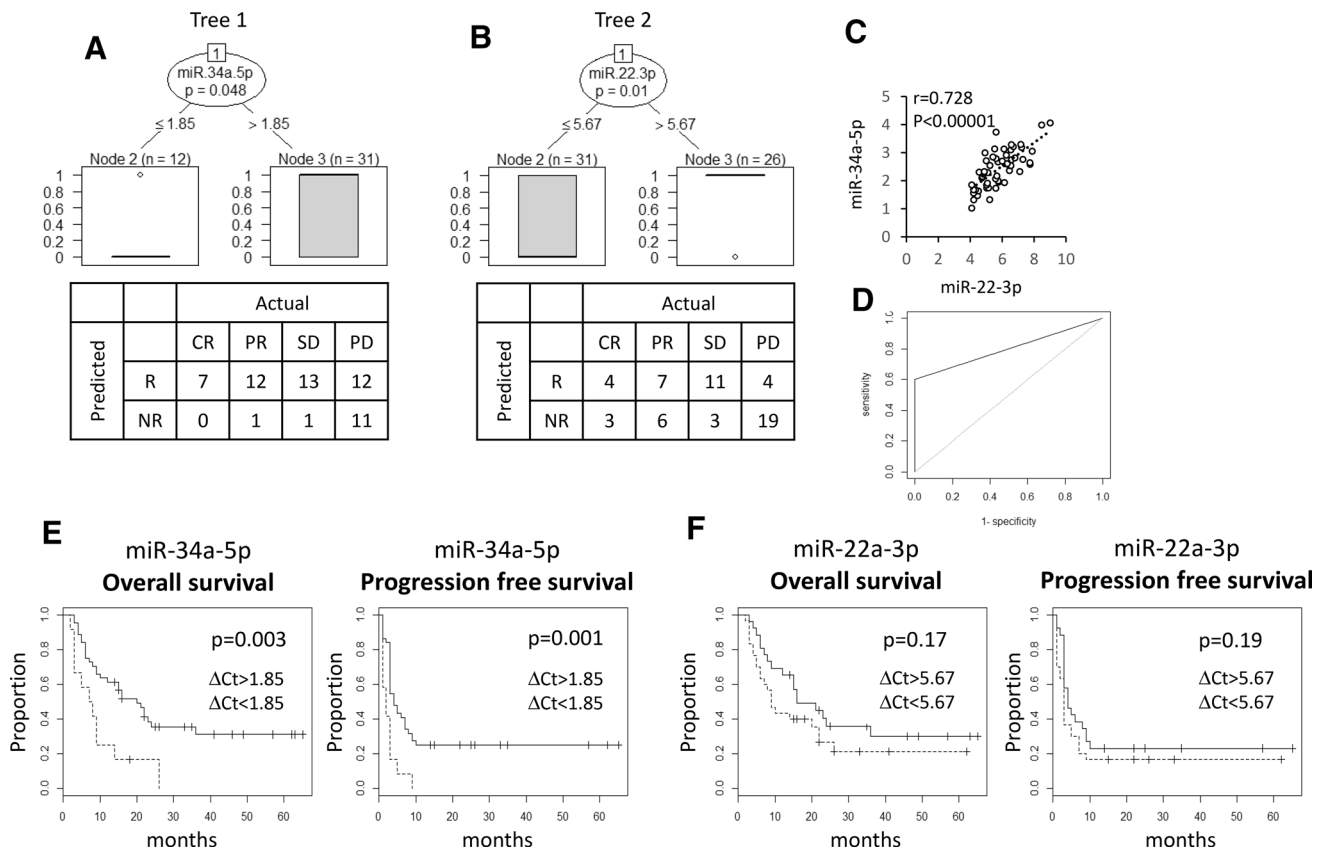


Fig. 4 miR-34a-5p and miR-22-3p expression predict response to TIL-ACT and overall survival. A classification tree with k-fold validation method was carried to distinguish Responders from Non-responders based on patients' **a** miR-34a-5p and **b** miR-22-3p expression levels. Both trees (1 and 2) fit the approaches of excluding SD patients from the classification analysis and re-adding them in the prediction stage and classifying SD patients together with CR+PR

patients as Clinical Benefit. **c** Correlation between miR-22-3p and miR-34a-5p expression in X and Y axes, respectively. Expression values are ΔCt . Pearson's r is shown. **d** Two-piece linear ROC curve determined by the proportions emanating from the classifications trees in **a**, **b**; **e**, **f** Kaplan-Meier analysis was performed on the terminal nodes of the best decision tree models. All p values were 2-sided and statistical significance was set at $p < 0.05$

by flow cytometry. CXCR3 and CD25 were expressed at similar levels (Fig. 5a). Next, the TIL cultures were tested for cytotoxic activity against autologous melanoma cells. Remarkably, and in line with the results depicted in Figs. 3 and 4, the miR-Low group exhibited a statistically significant higher cytotoxic activity than the miR-High group (Fig. 5b).

To test directly the effect of each microRNA, four Commercially available mimetics of miR-34a-5p, miR-22-3p, miR-34a-5p + miR-22-3p or non-targeting controls were electroporated into TIL14. TIL14 is comprised $> 97\%$ CD8(+) T cells. Expression levels of miR-34a-5p and miR-22-3p, which reflect the gene transfer efficiency, were confirmed by qRT-PCR (Fig. 5c). TILs over-expressing miR-34a-5p or miR-22-3p persistently showed reduced cytotoxicity ability by 30–35%, as compared to control (Fig. 5d). Co-transfection of miR-34a-5p and miR-22-3p inhibited cytotoxicity at levels similar to those observed when only one of the miRNAs was over-expressed. To be able to compare between treated cells, cytotoxicity levels

were normalized to the total number of TILs in each sample at the end of the assay. The calculated E:T in each well was between 2 and 3:1. Linearity of the cytotoxicity assay at different E:T ratios was confirmed (Fig. 5e). These results suggest that miR-34a-5p and miR-22-3p affect TILs cytotoxic activity and may serve as potential targets for improving TIL-ACT treatment. The full results for all individual experiments are depicted in Supplementary Table 3.

Phenotypic investigation of miR-High and miR-Low TIL cultures

The TIL cultures tested in Fig. 5B were analyzed for the expression of various cell surface markers, including immune checkpoints and activation markers, in addition to the markers described in Fig. 2 and Supplementary Table 1. Trends towards lower expression of CD28, and higher expression of CD27 and PD-1 were observed among the TIL cultures of the miR-Low group, as compared to the

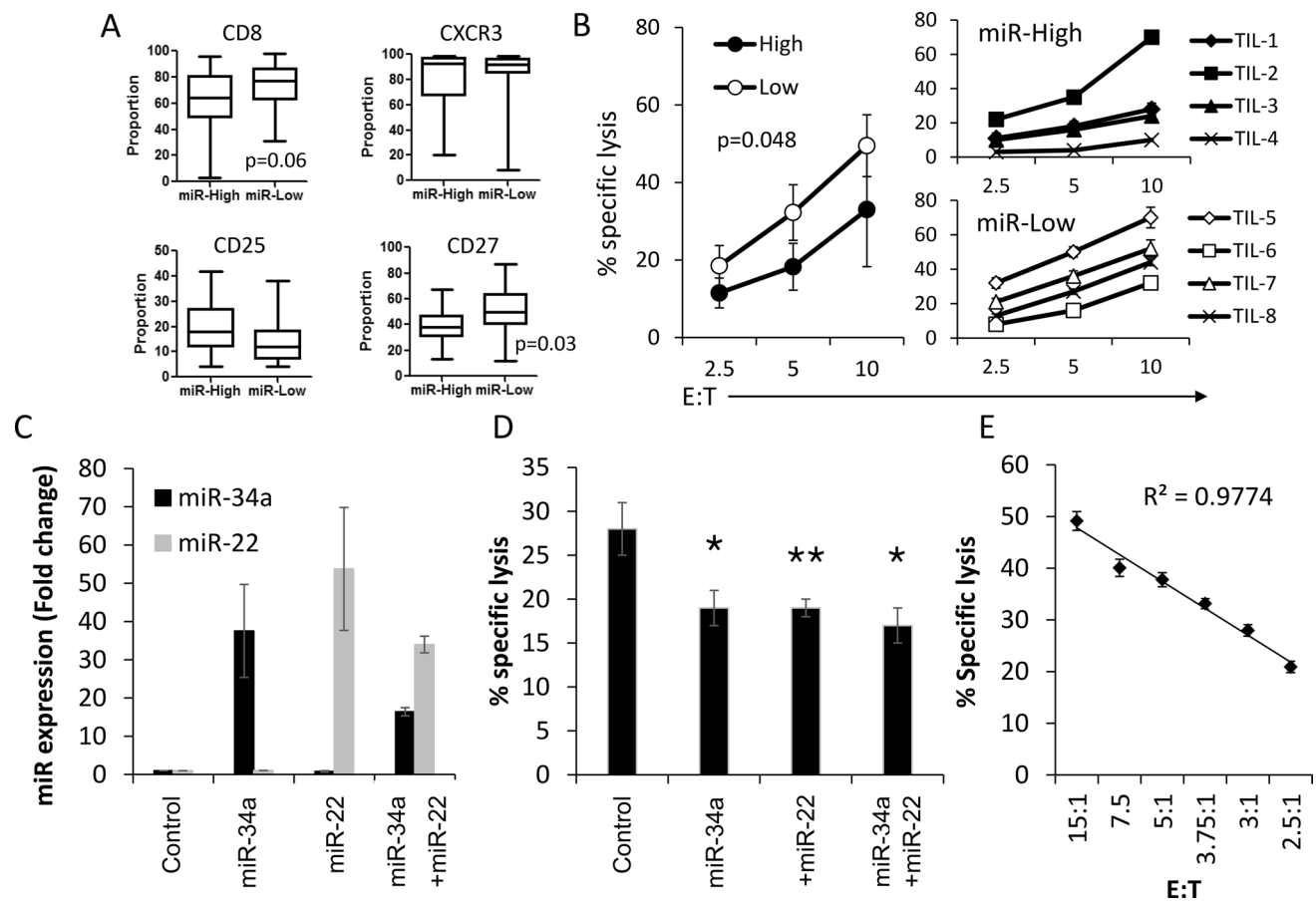


Fig. 5 miR-34a-5p and miR-22-3p regulate T-cell cytotoxicity. **a** Proportion of different markers among miR-High and miR-Low TIL cultures. **b** Specific killing of cognate melanoma cells by autologous TIL cultures from the miR-High or miR-Low groups. The left panel shows the average of all TIL cultures in each group. The right panel shows each individual TIL culture. X axis shows the Effector to Target ratio. **c** miR-34a-5p, miR-22-3p, both, or non-targeting mimics as control were electroporated into TIL14. Expression levels of miR-34a-5p and miR-22-3p was assessed by qRT-PCR and normalized to SNORD48

expression. **d** 72 h following electroporation, mel14 cells were added to TILs and co-incubated for 18 h. Specific lysis of melanoma cells was assessed by LDH release. **(E)** Different numbers of mel14 cells were co-incubated with fixed numbers of TIL14 for 18 h. Specific lysis of melanoma cells was assessed by LDH release and linearity of the cytotoxicity assay at different E:T ratios was assessed by R^2 . Experiments were performed three times in quadruplicates. E:T stands for Effector to Target. *Denotes $p < 0.05$, **denotes $p < 0.01$

miR-High group (Fig. 6a). The other tested markers did not exhibit any significant differences.

Next, RNA sequencing analysis was performed on seven of the TIL cultures (all but TIL-6). To better characterize the T-cell states of miR-High and -Low TIL products, we examined gene expression of inhibitory and stimulatory immune checkpoints, cytolytic genes and naïve T-cell markers (Fig. 6b, Supplementary Table 4). Differential gene expression analysis revealed upregulation of the stimulatory checkpoints CD28 ($p = 0.04$) and ICOS ($p = 0.04$) in the miR-High group, whereas the inhibitory checkpoint LAG3 ($p = 0.001$), the stimulatory checkpoint CD27 ($p = 0.04$) and the cytolytic score ($p = 0.05$) were upregulated in the miR-Low group (Supplementary Table 5).

Discussion

Several prognostic factors have been suggested for predicting response to TIL ACT, including number of cells infused, percentage of CD8 + CTL, specific T-cell subtypes and markers following co-incubation of TIL and tumor cells such as IFN- γ secretion [41]. Whereas the role of several miRNAs in T-cell biology was studied extensively [42, 43], their potential as predictors of response to cancer immunotherapy was hardly tested. Most efforts to identify predictive miRNAs signatures to cancer immunotherapy have focused on cancer cell-derived miRNAs, such as miR-222 that differentiates between patients with and without clinical benefit from Ipilimumab [33].

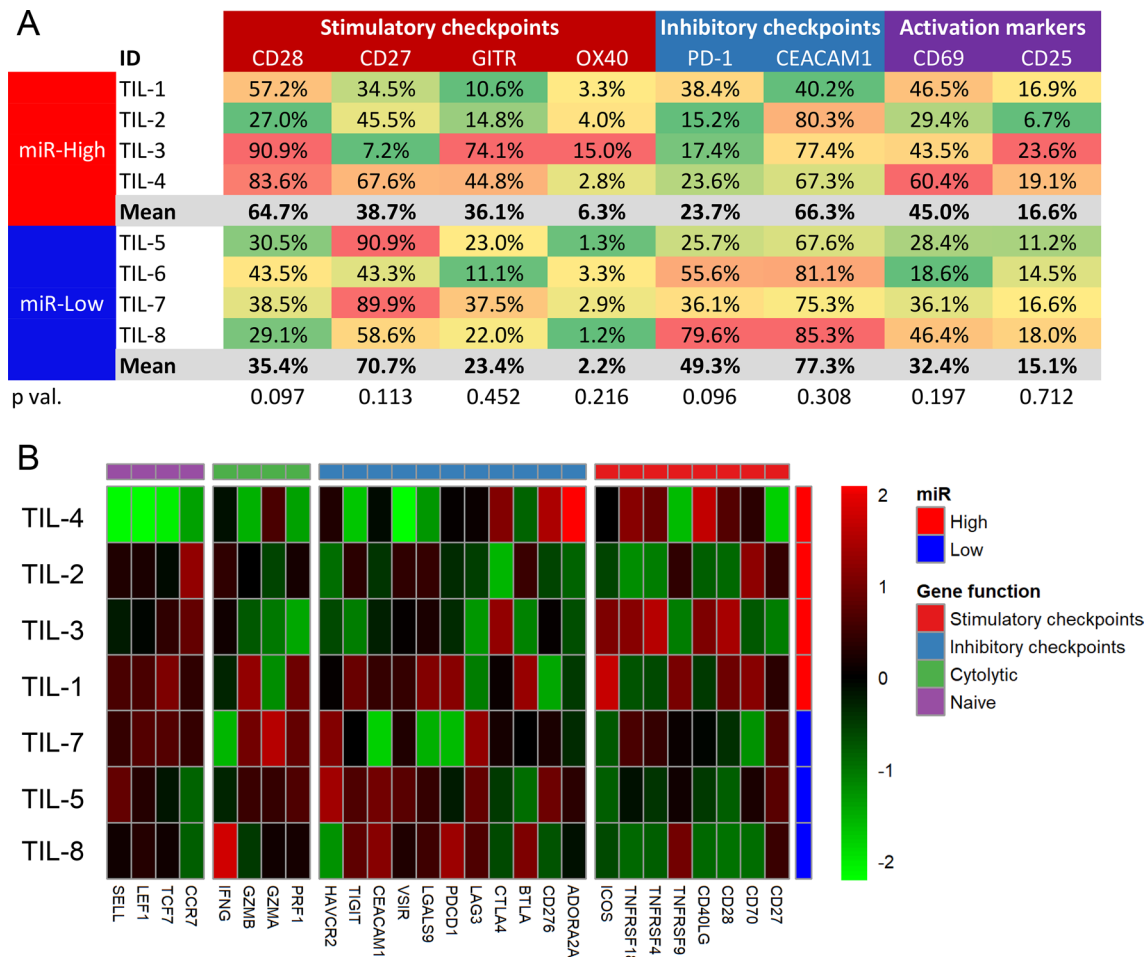


Fig. 6 Phenotypic and transcriptomic analyses of TIL cultures. Immune phenotyping and gene expression of inhibitory and stimulatory immune checkpoints, cytolytic genes and naïve T-cell markers in TIL cultures categorized by miR-Group. **a** Heat-map of TIL expression of various cell surface markers, as measured by flow cytometry. Values denote the percentage of positive TIL cells in each culture

with visual color scaling (red is high, green is low). The cell surface markers are indicated. Statistical significance was assessed with Student's *t* test; **b** heat-map of selected genes representing major T-cell status, as indicated in the figure, as measured by RNA sequencing of the transcriptome of TIL products. The statistical analysis is available in Supplementary Table 5

Here we identified a specific miRNA signature within the TILs, affecting effectors function and not the tumor, which is strongly associated with response to TIL-ACT treatment. miR-22-3p and miR-34a-5p were differentially expressed between patients who responded to TIL-ACT and those whose disease progressed despite the treatment. Importantly, the expression of miR-34a-5p and miR-22-3p in SD patients was similar to their expression in the responders group (Fig. 3a). Of note, although previous studies showed higher percentage of CD8 + T cells in responders compared to non-responders patients [17, 19], no correlation was observed between the percentage of CD8 + T cells and the expression levels of these miRNAs (Supplementary Fig. 2). This implies that the difference in miRNAs expression observed between the groups in this study is not due to differences in the proportion of CD8 + cells.

Classification models classified SD patients as responders, rather than non-responders (Fig. 4). The Disease Control Rate is a measure that collates CR, PR and SD, and is commonly reported in clinical trials, as SD can still confer survival benefit. In our cohort, the PFS of SD patients was more similar to the PFS of PD patients, but nevertheless, the overall survival of SD patients was dramatically different than that of PD patients (Fig. 2). There were no significant differences between the groups regarding subsequent therapies (Table 1). Although both miRNAs could predict response to TIL-ACT treatment, only miR-34a-5p was associated with better OS and PFS in these patients, while miR-22-3p expression showed no association. This may be due to additional, potential relevant effects of miR-34a.

The potential effect of miR-34a-5p and miR-22-3p on TIL activity was tested as a proof of concept by cytotoxicity

assays. TIL cultures with high expression of the microRNAs exhibited reduced cytotoxic activity as compared to those with low microRNA expression. These two miRs were mostly co-expressed in our dataset (Fig. 4c). TIL from the miR-High group exhibited lower killing activity than the TIL from the miR-Low group (Fig. 5b). Phenotypic analysis of these cultures point on a trend for higher PD-1 and CD27, as well as lower CD28 expression among the miR-Low group (Fig. 6a). RNA sequencing confirmed the differences in CD27 and CD28, and further added higher expression of LAG3 and overall cytolytic score among the miR-Low group (Fig. 6b and Supplementary Table 5). The combined transcription and immune phenotyping analyses concur with each other, as well with the functional cytotoxicity results. High PD-1 expression is indicative of terminally exhausted T cells [44], which are known to co-express Tim-3 and Lag-3 [45] and exhibit higher cytotoxic activity [46]. Thus, it could be speculated that the low expression of miR-34a-5p and miR-22-3p is associated, or could contribute to, the T-cell status of terminal effector differentiation. The main limitation is the low number of analyzed cultures.

Moreover, direct transfection of these miRNAs induced a reduction in cytotoxicity capacity *in vitro* (Fig. 5c, d). These results could partially explain the clinical outcome of PD patients who express higher levels of these miRNAs. Co-expression of both miRNAs did not demonstrate additive or synergistic effect over each of the individual miRNAs, suggesting an effect through the same pathway, acting redundantly. These results are in accordance with the high correlation between these miRNAs as well as with the classification trees of miR-34a-5p and miR-22-3p, which are interchangeable (Fig. 4a, b).

miR-34a, a direct target of p53, is a well-known tumor suppressor which is inactivated in many cancers [47]; however, its contribution to CD8+ T-cell biology is largely unknown. miR-22 is ubiquitously expressed in various tissues and can act both as a tumor suppressor and an oncogene in various cell types [48], and like miR-34a, its role in T-cell biology is largely unknown. Cobb et al. showed that miR-22 is preferentially expressed in regulatory T cells compared to conventional CD4 T cells [49]. We, therefore, used TargetScan and Toppgene (<https://toppgene.cchmc.org/enrichment.jsp>) algorithms to find predicted targets and pathways (Supplementary Fig. 3). Our analysis proposes two general pathways – TGF- β pathway and Notch signaling. Both pathways have been reported to be immune regulators. It was shown that Notch signaling controls IFN- γ production of naïve and effector T cells, and whereas it is crucial for lytic functions of naïve T cells, it is not required for the cytolytic activity of established effector CD8+ cells [50]. *In vivo* studies showed a critical role for Notch1 and Notch2 in antitumor CD8+ T-cell responses and suggested the use of transgenic-Notch1 intracellular domain in activated CD8+ T cells to

improve immunotherapy efficacy [51]. TGF- β controls immune homeostasis by regulating activation, proliferation, differentiation and function of many immune cell types. Several studies have shown that TGF- β suppresses CD8+ T-cell activation, proliferation and cytotoxicity, thus promoting tumor immune escape [52]. It is still unclear what is the total effect of the microRNAs on the TGF β pathway output, and it remains to be investigated.

Overall, this work suggests that miR-34a-5p and miR-22-3p may serve as biomarkers for predicting response to TIL-ACT. Larger independent series are warranted to confirm these results. The ability to predict response prior to administration of TIL will minimize ineffective treatment, thereby reducing costs and patients' suffer. The drawback of this study is the use of TILs from the final infusion bag. Future prospective analyses could be performed with TILs prior to their *ex vivo* expansion or at least during days 6-7 or the rapid expansion process. This could aid the Go/No-Go decision whether to continue with the pre-conditioning regimen with high dose chemotherapy.

Acknowledgements The authors would like to thank the Aronson Fund and the Lemelbaum family fund for their generous support. G.M is supported by the Melanoma Research Alliance Saban Family Team Sciences Award, Samueli Foundation Grant for Integrative Immunology and Israel Science Foundation Grant 15/1925.

Compliance with ethical standards

Conflict of interest The authors state no conflict of interest.

References

1. Sang M, Wang L, Ding C, Zhou X, Wang B, Lian Y, Shan B (2011) Melanoma-associated antigen genes - an update. *Cancer Lett* 302:85–90. [https://doi.org/S0304-3835\(10\)00506-9](https://doi.org/S0304-3835(10)00506-9)
2. Lawrence MS, Stojanov P, Polak P et al (2013) Mutational heterogeneity in cancer and the search for new cancer-associated genes. *Nature* 499:214–218. <https://doi.org/10.1038/nature12213>
3. Zikich D, Schachter J, Besser MJ (2013) Immunotherapy for the management of advanced melanoma: the next steps. *Am J Clin Dermatol* 14:261–272. <https://doi.org/10.1007/s40257-013-0013-0>
4. Lee C, Collichio F, Ollila D, Moschos S (2013) Historical review of melanoma treatment and outcomes. *Clin Dermatol* 31:141–147. <https://doi.org/10.1016/j.clindermatol.2012.08.015s0738-081x>
5. Hodi FS, O'Day SJ, McDermott DF et al (2010) Improved survival with ipilimumab in patients with metastatic melanoma. *N Engl J Med* 363:711–723. <https://doi.org/10.1056/nejmoa1003466>
6. Robert C, Thomas L, Bondarenko I et al (2011) Ipilimumab plus dacarbazine for previously untreated metastatic melanoma. *N Engl J Med* 364:2517–2526. <https://doi.org/10.1056/nejmoa1104621>
7. Robert C, Long GV, Brady B et al (2014) Nivolumab in Previously Untreated Melanoma without BRAF Mutation. *N Engl J Med*. <https://doi.org/10.1056/nejmoa1412082>
8. Robert C, Schachter J, Long GV et al (2015) Pembrolizumab versus Ipilimumab in Advanced Melanoma. *N Engl J Med* 372:2521–2532. <https://doi.org/10.1056/nejmoa1503093>

9. Larkin J, Chiarion-Sileni V, Gonzalez R et al (2015) Combined Nivolumab and Ipilimumab or Monotherapy in Untreated Melanoma. *N Engl J Med* 373:23–34. <https://doi.org/10.1056/nejmoa1504030>
10. Margolis N, Markovits E, Markel G (2019) Reprogramming lymphocytes for the treatment of melanoma: from biology to therapy. *Adv Drug Deliv Rev* 141:104–124
11. Markel G, Seidman R, Stern N et al (2006) Inhibition of human tumor-infiltrating lymphocyte effector functions by the homophilic carcinoembryonic cell adhesion molecule 1 interactions. *J Immunol* 177:6062–6071. <https://doi.org/10.1172/JCI27662>
12. Ortenberg R, Sapir Y, Raz L et al (2012) Novel Immunotherapy for Malignant Melanoma with a Monoclonal Antibody That Blocks CEACAM1 Homophilic Interactions. *Mol Cancer Ther* 11:1300–1310. <https://doi.org/10.1158/1535-7163>
13. Rosenberg SA, Dudley ME (2009) Adoptive cell therapy for the treatment of patients with metastatic melanoma. *Curr Opin Immunol* 21:233–240. [https://doi.org/S0952-7915\(09\)00025-9](https://doi.org/S0952-7915(09)00025-9)
14. Besser MJ, Shapira-Frommer R, Treves AJ et al (2009) Minimally cultured or selected autologous tumor-infiltrating lymphocytes after a lympho-depleting chemotherapy regimen in metastatic melanoma patients. *J Immunother* 32:415–423. <https://doi.org/10.1097/cji.0b013e31819c8bda00002371>
15. Dudley ME, Wunderlich JR, Shelton TE, Even J, Rosenberg SA (2003) Generation of tumor-infiltrating lymphocyte cultures for use in adoptive transfer therapy for melanoma patients. *J Immunother* 26:332–342
16. Tran KQ, Zhou J, Durflinger KH, Langhan MM, Shelton TE, Wunderlich JR, Robbins PF, Rosenberg SA, Dudley ME (2008) Minimally cultured tumor-infiltrating lymphocytes display optimal characteristics for adoptive cell therapy. *J Immunother* 31:742–751. <https://doi.org/10.1097/cji.0b013e31818403d500002371>
17. Besser MJ, Shapira-Frommer R, Itzhaki O et al (2013) Adoptive Transfer of Tumor Infiltrating Lymphocytes in Metastatic Melanoma Patients: intent-to-Treat Analysis and Efficacy after Failure to Prior Immunotherapies. *Clin Cancer Res* 19:4792–4800. <https://doi.org/1078-0432.CCR-13-0380>
18. Rosenberg SA, Yang JC, Sherry RM et al (2011) Durable complete responses in heavily pretreated patients with metastatic melanoma using T-cell transfer immunotherapy. *Clin Cancer Res* 17:4550–4557. <https://doi.org/10.1158/1078-0432.ccr-11-01161078-0432>
19. Radvanyi LG, Bernatchez C, Zhang M et al (2012) Specific lymphocyte subsets predict response to adoptive cell therapy using expanded autologous tumor-infiltrating lymphocytes in metastatic melanoma patients. *Clin Cancer Res* 18:6758–6770. <https://doi.org/10.1158/1078-0432.ccr-12-11771078-0432>
20. Bartel DP (2004) MicroRNAs: genomics, biogenesis, mechanism, and function. *Cell* 116:281–297. <https://doi.org/S0092867404000455>
21. Kim VN, Nam JW (2006) Genomics of microRNA. *Trends Genet* 22:165–173. [https://doi.org/S0168-9525\(06\)00021-7](https://doi.org/S0168-9525(06)00021-7)
22. Wojcicka A, de la Chapelle A, Jazdzewski K (2013) MicroRNA-related sequence variations in human cancers. *Hum Genet*. <https://doi.org/10.1007/s00439-013-1397-x>
23. Friedman RC, Farh KK, Burge CB, Bartel DP (2009) Most mammalian mRNAs are conserved targets of microRNAs. *Genome Res* 19:92–105. <https://doi.org/10.1101/gr.082701.108>
24. O'Connell RM, Rao DS, Chaudhuri AA, Baltimore D (2010) Physiological and pathological roles for microRNAs in the immune system. *Nat Rev Immunol* 10:111–122. <https://doi.org/10.1038/nri2708>
25. Basak I, Patil KS, Alves G, Larsen JP, Moller SG (2015) microRNAs as neuroregulators, biomarkers and therapeutic agents in neurodegenerative diseases. *Cell Mol Life Sci*. <https://doi.org/10.1007/s00018-015-2093>
26. Pencheva N, Tavazoie SF (2013) Control of metastatic progression by microRNA regulatory networks. *Nat Cell Biol* 15:546–554. <https://doi.org/10.1038/ncb2769ncb2769>
27. Di Leva G, Croce CM (2013) miRNA profiling of cancer. *Curr Opin Genet Dev* 23:3–11. <https://doi.org/10.1016/j.gde.2013.01.004s0959-437x>
28. Iorio MV, Croce CM (2012) microRNA involvement in human cancer. *Carcinogenesis* 33:1126–1133. <https://doi.org/10.1093/carcin/bgs140bgs140>
29. Hayes J, Peruzzi PP, Lawler S (2014) MicroRNAs in cancer: biomarkers, functions and therapy. *Trends Mol Med*. 20:460–469. <https://doi.org/10.1016/j.molmed.2014.06.005>
30. Nana-Sinkam SP, Croce CM (2013) Clinical applications for microRNAs in cancer. *Clin Pharmacol Ther* 93:98–104. <https://doi.org/10.1038/clpt.2012.192>
31. Itzhaki O, Hovav E, Ziporen Y et al (2011) Establishment and large-scale expansion of minimally cultured “young” tumor infiltrating lymphocytes for adoptive transfer therapy. *J Immunother* 34:212–220. <https://doi.org/10.1097/cji.0b013e318209c94c>
32. Besser MJ, Shapira-Frommer R, Treves AJ et al (2010) Clinical responses in a phase II study using adoptive transfer of short-term cultured tumor infiltration lymphocytes in metastatic melanoma patients. *Clin Cancer Res* 16:2646–2655. <https://doi.org/10.1158/1078-0432.ccr-10-0041078-0432>
33. Galore-Haskel G, Nemlich Y, Greenberg E et al. (2015) A novel immune resistance mechanism of melanoma cells controlled by the ADAR1 enzyme. *Oncotarget*. 6: 28999-9015. <https://doi.org/10.18632/oncotarget.4905>
34. Dobin A, Davis CA, Schlesinger F, Drenkow J, Zaleski C, Jha S, Batut P, Chaisson M, Gingeras TR (2013) STAR: ultrafast universal RNA-seq aligner. *Bioinformatics* 29:15–21. <https://doi.org/10.1093/bioinformatics/bts635>
35. Liao Y, Smyth GK, Shi W (2014) FeatureCounts: an efficient general purpose program for assigning sequence reads to genomic features. *Bioinformatics* 30:923–930
36. Law CW, Chen Y, Shi W, Smyth GK (2014) Voom: precision weights unlock linear model analysis tools for RNA-seq read counts. *Genome Biol* 15:R29. <https://doi.org/10.1186/gb-2014-15-2-r29>
37. Ritchie ME, Phipson B, Wu D, Hu Y, Law CW, Shi W, Smyth GK (2015) Limma powers differential expression analyses for RNA-seq and microarray studies. *Nucleic Acids Res* 43:e47. <https://doi.org/10.1093/nar/gkv007>
38. Rooney MS, Shukla SA, Wu CJ, Getz G, Hacohen N (2015) Molecular and genetic properties of tumors associated with local immune cytolytic activity. *Cell* 160:48–61. <https://doi.org/10.1016/j.cell.2014.12.033>
39. Hothorn T, Hornik K, Zeileis A (2006) Unbiased recursive partitioning: a conditional inference framework. *Journal of Computational and Graphical statistics*. 15:651–674
40. Shmueli G, Bruce P, Yahav I, Petal R, Lichtendahl KC (2017) Data mining for business intelligence: Concepts, techniques, and applications in R.. 1st ed. John Wiley and Sons
41. Zikich D, Schachter J, Besser MJ (2016) Predictors of tumor-infiltrating lymphocyte efficacy in melanoma. *Immunotherapy*. 8:35–43. <https://doi.org/10.2217/imt.15.99>
42. Ji Y, Hocker JD, Gattinoni L (2015) Enhancing adoptive T cell immunotherapy with microRNA therapeutics. *Semin Immunol*. [https://doi.org/S1044-5323\(15\)00100-1](https://doi.org/S1044-5323(15)00100-1)
43. Jeker LT, Bluestone JA (2013) MicroRNA regulation of T-cell differentiation and function. *Immunol Rev* 253:65–81. <https://doi.org/10.1111/imr.12061>
44. Paley MA, Kroy DC, Odorizzi PM et al (2012) Progenitor and terminal subsets of CD8+ T cells cooperate to contain chronic

- viral infection. *Science* 338:1220–1225. <https://doi.org/10.1126/science.1229620>
45. Thommen DS, Koelzer VH, Herzig P et al (2018) A transcriptionally and functionally distinct PD-1 + CD8 + T cell pool with predictive potential in non-small-cell lung cancer treated with PD-1 blockade. *Nat Med* 24:994–1004. <https://doi.org/10.1038/s41591-018-0057-z>
 46. LaFleur MW, Nguyen TH, Coxe MA et al (2019) PTPN2 regulates the generation of exhausted CD8 + T cell subpopulations and restrains tumor immunity. *Nat Immunol* 20:1335–1347. <https://doi.org/10.1038/s41590-019-0480-4>
 47. Agostini M, Knight RA (2014) miR-34: from bench to bedside. *Oncotarget*. 5: 872–81. doi: 1825 [pii] <https://doi.org/10.18632/oncotarget.1825>
 48. Xiong J (2012) Emerging roles of microRNA-22 in human disease and normal physiology. *Curr Mol Med* 12:247–258. <https://doi.org/CMM-EPub-201201190201-005>
 49. Cobb BS, Hertweck A, Smith J et al (2006) A role for Dicer in immune regulation. *J Exp Med* 203:2519–2527. <https://doi.org/jem.20061692>
 50. Kuijk LM, Verstege MI, Rekers NV, Bruijns SC, Hooijberg E, Roep BO, de Gruijl TD, van Kooyk Y, Unger WW (2013) Notch controls generation and function of human effector CD8 + T cells. *Blood* 121:2638–2646. <https://doi.org/10.1182/blood-2012-07-442962>
 51. Sierra RA, Thevenot P, Raber PL, Cui Y, Parsons C, Ochoa AC, Trillo-Tinoco J, Del Valle L, Rodriguez PC (2014) Rescue of notch-1 signaling in antigen-specific CD8 + T cells overcomes tumor-induced T-cell suppression and enhances immunotherapy in cancer. *Cancer Immunol Res* 2:800–811. <https://doi.org/10.1158/2326-6066>
 52. Yang L, Pang Y, Moses HL (2010) TGF-beta and immune cells: an important regulatory axis in the tumor microenvironment and progression. *Trends Immunol* 31:220–227. <https://doi.org/10.1016/j.it.2010.04.002>

Publisher's Note Springer Nature remains neutral with regard to jurisdictional claims in published maps and institutional affiliations.